Journal of Enzyme Inhibition and Medicinal Chemistry, 2011; 26(2): 245–253

ISSN 1475-6366 print/ISSN 1475-6374 online
DOI: 10.3109/14756366.2010.496362

informa
healthcare

RESEARCH ARTICLE

The preparation, *in vitro* screening and molecular docking of symmetrical bisquaternary cholinesterase inhibitors containing a but-(2E)-en-1,4-diyl connecting linkage

Kamil Musilek[1,4], Ruzena Pavlikova[1], Jan Marek[1], Marketa Komloova[2], Ondrej Holas[2], Martina Hrabinova[3], Miroslav Pohanka[3], Vlastimil Dohnal[4], Martin Dolezal[2], Frank Gunn-Moore[5], and Kamil Kuca[3,4]

[1]University of Defence, Faculty of Military Health Sciences, Department of Toxicology, Trebesska 1575, Hradec Kralove, Czech Republic, [2]Charles University, Faculty of Pharmacy, Department of Pharmaceutical Chemistry and Drug Control, Heyrovskeho 1203, Hradec Kralove, Czech Republic, [3]University of Defence, Faculty of Military Health Sciences, Centre of Advanced Studies, Trebesska 1575, Hradec Kralove, Czech Republic, [4]University of Jan Evangelista Purkynje, Faculty of Science, Department of Chemistry, Ceske mladeze 8, Usti nad Labem, Czech Republic, and [5]University of St. Andrews, School of Biology, Bute Building, St. Andrews, Fife, UK

Abstract

Carbamate inhibitors (e.g. pyridostigmine bromide) are used as a pre-treatment for the prevention of organophosphorus poisoning. They work by blocking the native function of acetylcholinesterases (AChE) and thus protect AChE against irreversible inhibition by organophosphorus compounds. However, carbamate inhibitors are known for their many undesirable side effects related to the carbamylation of AChE. In this paper, we describe 17 novel bisquaternary compounds and have analysed their effect on AChE inhibition. The newly prepared compounds were evaluated *in vitro* using both human erythrocyte AChE and human plasmatic butyrylcholinesterase. Their inhibitory ability was expressed as the half maximal inhibitory concentration (IC_{50}) and then compared to the standard carbamate drugs and two AChE reactivators. One of these novel compounds showed promising AChE inhibition *in vitro* (nM range) and was better than the currently used standards. Additionally, a kinetic assay confirmed the non-competitive inhibition of hAChE by this novel compound. Consequently, the docking results confirmed the apparent π-π or π-cationic interactions with the key amino acid residues of hAChE and the binding of the chosen compound at the enzyme catalytic site.

Keywords: Cholinesterase, inhibitor, pre-treatment, myasthenia gravis, quaternary, in vitro, docking

Introduction

Acetylcholinesterase (AChE; E.C. 3.1.1.7) inhibitors are compounds which have been of interest for several decades. They are used for the treatment of neurodegenerative diseases such as Alzheimer's disease or myasthenia gravis [1–2]. In addition, some AChE inhibitors are used as pre-exposure drugs to protect against organophosphorus poisonings, such as nerve agents [3].

Generally, the organophosphorus (OP) compounds (e.g. nerve agents and pesticides) are lethal, causing irreversible inhibition of AChE [4]. Consequently, acetylcholine accumulates on the synaptic junctions and this excess causes permanent stimulation of the muscarinic or nicotinic receptors. Gradually, the stimulation of the receptors leads to a cholinergic crisis and death by malfunction of the muscles associated with breathing control [5]. Among the OP compounds, nerve agents are among the most toxic compounds that have been developed by man. There are several methods to counteract the toxicity of nerve agents [5] either involving a pre-exposure or post-exposure approach. Reversible AChE inhibitors, stoichiometric and catalytic scavengers can be used as a pre-exposure strategy

Address for Correspondence: Kamil Musilek, Department of Toxicology, Faculty of Military Health Sciences, Trebesska 1575, Hradec Kralove, Czech Republic. E-mail: musilek@pmfhk.cz; Tel: +420-973-251-523; Fax: +420-495-518-094

(Received 08 February 2010; revised 18 May 2010; accepted 24 May 2010)

[6], whilst a post-exposure treatment usually consists of a combination of an anticholinergic drug, AChE reactivator and an anticonvulsant such as diazepam [5].

With regard to the pre-exposure strategies, the only method currently allowed for human use is based on reversible AChE inhibitors (usually carbamates, e.g. pyridostigmine bromide, neostigmine bromide; **1**–**2**; Figure 1) in combination with anticholinergic drugs (e.g. benactyzine, trihexyphenidyl) to antagonise the effects of the accumulated acetylcholine [7]. The carbamates reversibly inhibit AChE, protect the enzyme against inhibition by OP and are spontaneously decarbamylated with normal restoration of AChE activity [8]. However, although carbamates are widely used, they are known for many side effects including gastrointestinal effects (nausea, intestinal obstruction), increased bronchial secretion, cardiac arrhythmia or a cholinergic crisis [9–10].

The most widely used carbamate for OP pre-treatment is pyridostigmine (**1**) [7]. Its charged molecule has poor penetration of the blood-brain barrier (BBB) and probably cannot protect brain AChE, but the pre-treatment effect is ensured by use of anticholinergic drugs (benactyzine, trihexyphenidyl) [11]. On account of its serious side effects, a carbamate inhibitor **1** in combined pre-treatment strategies, can be replaced by other reversible inhibitors (e.g. hupezine A) [7]. The advantage of such reversible cholinesterase inhibitors should be its selectivity for AChE, where butyrylcholinesterase (BChE; EC 3.1.1.8) can act as a physiological scavenger of OP. Decreasing the side effects of a new reversible inhibitor would also be an advantage if it does not directly affect the AChE active site (S203). However, there remains the problem of BBB penetration that can be overcome by anticholinergic drugs (benactyzine, trihexyphenidyl) thereby without increasing toxicity from the reversible AChE inhibitor.

Due to these necessary improvements for protecting against OP, a series of symmetrical bisquaternary compounds bearing (2*E*)-buten-1,4-diyl linkage were synthesised to potentially replace pyridostigmine for the combined pre-exposure strategy. The quaternary compounds (e.g. AChE reactivators) are also known to be receptor acting drugs [12]. Many of them were found to be potent activators, competitive antagonists or non-competitive blockers of muscarinic or nicotinic receptors. However, their effects on receptors cannot be accurately predicted and the quaternary origin of these novel compounds might help to increase protection against OP [12].

The design of novel compounds (**5**–**21**; Figure 2) originated from AChE reactivators (e.g. pralidoxime, K203; **3**–**4**), especially those bearing the same but-(2*E*)-en-1,4-diyl linkage (**4**), that had been previously found to protect against OP exposure both *in vitro* and *in vivo* [13–15]. Essentially, the core part of the newly prepared molecules remained consistent with former AChE reactivators including a but-(2*E*)-en-1,4-diyl linkage and two pyridinium rings. The oxime moieties on both pyridinium rings were changed and a broad variety of functional groups were added. The functional groups were chosen as representatives of lipophilic (Me, Ph) or hydrophilic (OH, COOH) moieties to assess the potential interactions with the enzyme's active site [16]. Specifically these were placed on the 4-position on the pyridinium ring as this was the most suitable for potential interactions within the narrow AChE cleft and so would hypothetically increase its inhibitory ability towards AChE [17].

All the new compounds were prepared using a standard synthetic strategy [18]. The solution containing the pyridine derivative (4.7 mmol) and 1,4-dibromobut-(2*E*)-ene (2.3 mmol) in dimethylformamide (DMF) (10 ml) was stirred at 70°C for 2 to 48 hours. Subsequently, the reaction mixture was cooled to room temperature. It was then portioned with acetone (50 ml) and again cooled in a refrigerator (5°C) overnight. The crystalline or amorphous crude product was collected by filtration, washed with acetone (3 × 20 ml) and re-crystallised from MeCN [19]. NMR, ESI-MS and elemental analysis were used to determine the purity of all the compounds.

Material and methods

Chemistry

Solvents (acetone, DMF, MeCN) and reagents were purchased from Fluka (Prague, Czech Republic) and Sigma-Aldrich (Prague, Czech Republic) and used without further purification. Reactions were monitored by TLC using DC-Alufolien Cellulose F (Darmstadt, Merck, Germany) and a mobile phase of BuOH-CH_3COOH-H_2O 5:1:2, detection by solution of Dragendorff reagent (solution containing 10 mL CH_3COOH, 50 mL H_2O and 5 mL of basic solution prepared by mixing of two fractions – fraction A: 850 mg $Bi(NO_3)_3$, 40 mL H_2O, 10 mL CH_3COOH; fraction B: 8 g KI, 20 mL H_2O). Melting points were measured on a micro heating stage PHMK 05 (VEB Kombinat Nagema, Radebeul, Germany) and were uncorrected.

NMR spectra were generally recorded using a Varian Gemini 300 (^1H 300 MHz, ^{13}C 75 MHz, Palo Alto CA, USA).

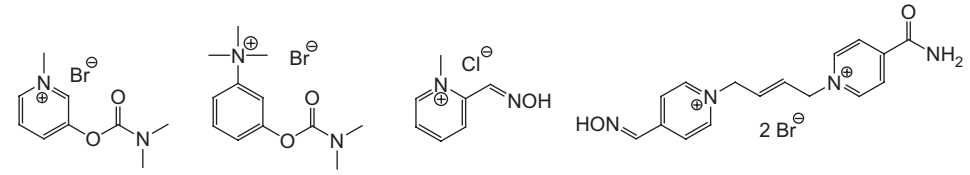

Figure 1. Selected acetylcholinesterase inhibitors and reactivators.

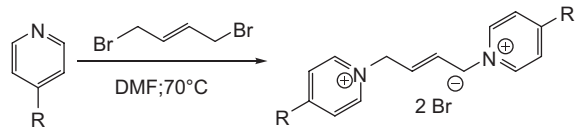

5, R = Me

6, R = Et

7, R = *tert.*-Bu

8, R = Ph

9, R = Bn

10, R = $(CH_2)_3Ph$

11, R = 4-NO_2-Bn

12, R = OH

13, R = CH_2OH

14, R = $(CH_2)_3OH$

15, R = $N(CH_3)_2$

16, R = CH=NOH

17, R = $COCH_3$

18, R = COOH

19, R = $COOCH_3$

20, R = $CONH_2$

21, R = CN

Figure 2. Prepared bisquaternary pyridinium salts.

In all cases, the chemical shift values for ^{1}H spectra were reported in ppm (δ) relative to residual $CHD_2SO_2CD_3$ (δ 2.5) or D_2O (δ 4.79), shift values for ^{13}C spectra are reported in ppm (δ) relative to solvent peak dimethylsulphoxide - d_6 δ 39.43. Signals are quoted as s (singlet), d (doublet), t (triplet) and m (multiplet).

The mass spectra (MS respectively MSn) were measured on a LCQ FLEET ion trap and evaluated using Xcalibur v 2.5.0 software (both Thermo Fisher Scientific, San Jose, CA, USA). The sample was dissolved in deionised water (Goro, Prague, Czech Republic) and injected continuously (8 ul/ min) by Hamilton syringe into the electrospray ion source. The parameters for the electrospray were set up as follows: sheath gas flow rate 20 arbitrary units, aux gas flow rate 5 arbitrary units, sweep gas flow rate 0 arbitrary units, spray voltage 5 kV, capillary temperature 275°C, capillary voltage 13 V, tube lens 100 V.

Prepared bisquaternary salts

but-(2E)-en-1,4-diyl-1,1′-bis(4-methylpyridinium) dibromide (5)

Mp 256–257°C. Yield 54%. ^{1}H NMR (300 MHz, DMSO d_6): δ (ppm) 8.71–8.67 (m, 4H, H–2,2′,6,6′), 8.08–8.04 (m, 4H, H–3,3′,5,5′), 6.17–6.12 (m, 2H, =*CH*-), 5.17–5.14 (m, 4H, -CH_2-), 3.65 (s, 6H, N-CH_3). ^{13}C NMR (75 MHz, DMSO d_6): δ (ppm) 150.26, 147.04, 145.84, 131.25, 126.01, 62.45. ESI-MS: *m/z* 239.9 [M^{2+}] (calculated for [$C_{16}H_{20}N_2^{2+}$] 240.16). EA: calculated 48.02% C, 5.04% H, 7% N; found 48.44% C, 4.87% H, 5.24% N.

but-(2E)-en-1,4-diyl-1,1′-bis(4-ethylpyridinium) dibromide (6)

Mp 227–228°C. Yield 49%. ^{1}H NMR (300 MHz, DMSO d_6): δ (ppm) 8.55 (d, 4H, *J* = 6.2 Hz, H–2,2′,6,6′), 7.96 (d, 4H, *J* = 6.2 Hz, H–3,3′,5,5′), 6.28–6.24 (m, 2H, =*CH*-), 5.30–5.25 (m, 4H, -CH_2-), 2.98 (m, 4H, -CH_2-CH_3), 1.31 (t, 6H, *J* = 7.4 Hz, -CH_3). ^{13}C NMR (75 MHz, DMSO d_6): δ (ppm) 142.78, 129.31, 127.08, 60.23, 27.93, 12.15. ESI-MS: *m/z* 268.1 [M^{2+}] (calculated for [$C_{18}H_{24}N_2^{2+}$] 268.19). EA: calculated 50.49% C, 5.65% H, 6.54% N; found 50.12% C, 5.56% H, 6.76% N.

but-(2E)-en-1,4-diyl-1,1′-bis(4-tert-butylpyridinium) dibromide (7)

Mp 235–237°C. Yield 66%. ^{1}H NMR (300 MHz, DMSO d_6): δ (ppm) 8.74 (d, 4H, *J* = 5.8 Hz, H–2,2′,6,6′), 8.12 (d, 4H, *J* = 5.8 Hz, H–3,3′,5,5′), 6.29–6.25 (m, 2H, =*CH*-), 5.31–5.27 (m, 4H, -CH_2-), 1.39 (s, 18H, CH_3-). ^{13}C NMR (75 MHz, DMSO d_6): δ (ppm) 142.82, 129.33, 125.02, 60.07, 35.46, 28.55. ESI-MS: *m/z* 324.1 [M^{2+}] (calculated for [$C_{22}H_{32}N_2^{2+}$] 324.26). EA: calculated 54.56% C, 6.66% H, 5.78% N; found 54.3% C, 6.76% H, 5.84% N.

but-(2E)-en-1,4-diyl-1,1′-bis(4-phenylpyridinium) dibromide (8)

Mp 259–261°C. Yield 55%. ^{1}H NMR (300 MHz, DMSO d_6): δ (ppm) 8.78–8.65 (m, 4H, H–2,2′,6,6′), 8.31–8.17 (m, 4H, H–3,3′,5,5′), 7.94–7.79 (m, 4H, Ph–2,2′,6,6′), 7.63–7.44 (m, 6H, Ph–3,3′,4,4′,5,5′), 6.23–6.12 (m, 2H, =*CH*-), 5.23–5.11 (m, 4H, -CH_2-). ^{13}C NMR (75 MHz, DMSO d_6): δ (ppm) 157.65, 157.63, 145.52, 134.73, 133.86, 131.25, 129.37, 126.19, 61.98. ESI-MS: *m/z* 364.2 [M^{2+}] (calculated for [$C_{26}H_{24}N_2^{2+}$] 364.19). EA: calculated 59.56% C, 4.61% H, 5.34% N; found 59.85% C, 4.4% H, 4.9% N.

but-(2E)-en-1,4-diyl-1,1′-bis(4-phenylmethylpyridinium) dibromide (9)

Mp 212–214°C. Yield 4%. ^{1}H NMR (300 MHz, DMSO d_6): δ (ppm) 9.32 (d, 2H, *J* = 6.1 Hz, H–2,6), 8.98 (d, 2H, *J* = 6.1 Hz, H–2′,6′), 8.41 (d, 2H, *J* = 6.1 Hz, H–3,5), 8.08 (d, 2H, *J* = 6.1 Hz, H–3′,5′), 7.94–7.77 (m, 3H, Ph), 7.72–7.58 (m, 2H, Ph), 7.44–7.23 (m, 5H, Ph), 6.43–6.12 (m, 2H, =*CH*-), 5.58–5.19 (m, 4H, N-CH_2-), 4.3 (s, 4H, Ph-CH_2-). ^{13}C NMR (75 MHz, DMSO d_6): δ (ppm) 151.98, 145.85, 144.48, 137.5, 134.84, 134.04, 130.24, 130.09, 129.97, 129.11, 129.05, 128.88, 127.67, 127.03, 126.87, 60.99, 60.13. ESI-MS: *m/z* 391 [M^{2+}-H] (calculated for [$C_{28}H_{28}N_2^{2+}$-H] 391.22). EA: calculated 60.89% C, 5.11% H, 5.07% N; found 60.28% C, 5.57% H, 5.67% N.

but-(2E)-en-1,4-diyl-1,1′-bis(4-(3-phenylpropyl)-pyridinium) dibromide (10)

Mp 204–206°C. Yield 43%. ^{1}H NMR (300 MHz, DMSO d_6): δ (ppm) 8.58 (d, 4H, *J* = 6.1 Hz, H–2,2′,6,6′), 7.79 (d, 4H, *J* = 6.1 Hz, H–3,3′,5,5′), 7.27–7.11 (m, 10H, Ph), 6.18–6.14 (m, 2H, =*CH*-), 5.23–5.19 (m, 4H, -CH_2-), 2.89 (t, 4H, *J* = 7.3

Hz, Pyr-CH_2-), 2.63 (t, 4H, J = 7.3 Hz, Ph-CH_2-), 2.06–1.94 (m, 4H, Pyr-CH_2-CH_2-). ^{13}C NMR (75 MHz, DMSO d_6): δ (ppm) 142.7, 141.24, 129.39, 128.28, 128.08, 127.72, 125.65, 60.3, 34.22, 33.94, 29.79. ESI-MS: *m/z* 447.9 [M^{2+}] (calculated for [$C_{32}H_{36}N_2^{2+}$] 448.29). EA: calculated 63.17% C, 5.96% H, 4.6% N; found 63.16% C, 6.22% H, 4.61% N.

but-(2E)-en-1,4-diyl-1,1′-bis(4-(4-nitrobenzyl)-pyridinium) dibromide (11)

Mp 248–249°C. Yield 81 %. ^{1}H NMR (300 MHz, DMSO d_6): δ (ppm) 8.62 (d, 4H, J = 6.1 Hz, H–2,2′,6,6′), 7.99–7.89 (m, 4H, H–3,3′,5,5′), 7.79 (d, 4H, J = 7 Hz, Ph–2,2′,6,6′), 7.37 (d, 4H, J = 7 Hz, Ph–3,3′,5,5′), 6.1–6.04 (m, 2H, =*CH*-), 5.18–5.03 (m, 4H, N-CH_2-), 4.28 (s, 4H, Ph-CH_2-). ^{13}C NMR (75 MHz, DMSO d_6): δ (ppm) 147.85, 146.03, 145.34, 131.82, 131.19, 129.63, 125.34, 62.22, 41.49. ESI-MS: *m/z* 482.3 [M^{2+}] (calculated for [$C_{28}H_{26}N_4O_4^{2+}$] 482.19). EA: calculated 52.36% C, 4.08% H, 8.72% N; found 52.53% C, 4.37% H, 8.36% N.

but-(2E)-en-1,4-diyl-1,1′-bis(4-hydroxypyridinium) dibromide (12)

Mp 258–260°C. Yield 53 %. ^{1}H NMR (300 MHz, DMSO d_6): δ (ppm) 8.48 (d, 4H, J = 6.4 Hz, H–2,2′,6,6′), 7.24 (d, 4H, J = 6.4 Hz, H–3,3′,5,5′), 6.24–6.12 (m, 2H, =*CH*-), 5.12–5.03 (m, 4H, -CH_2-). ^{13}C NMR (75 MHz, DMSO d_6): δ (ppm) 144.6, 128.96, 114.34, 58.81. ESI-MS: *m/z* 244.1 [M^{2+}] (calculated for [$C_{14}H_{16}N_2O_2^{2+}$] 244.12). EA: calculated 41.61% C, 3.99% H, 6.93% N; found 41.45% C, 4.35% H, 7.07% N.

but-(2E)-en-1,4-diyl-1,1′-bis(4-hydroxymethylpyridinium) dibromide (13)

Mp 210–212°C. Yield 48 %. ^{1}H NMR (300 MHz, D_2O d_6): δ (ppm) 8.76 (d, 4H, J=5.5 Hz, H–2,2′,6,6′), 8.03 (d, 4H, J=5.8 Hz, H–3,3′,5,5′), 6.27–6.22 (m, 2H, =*CH*-), 5.33–5.27 (m, 4H, -CH_2-), 4.96 (s, 4H, -CH_2-OH). ^{13}C NMR (75 MHz, D_2O): δ (ppm) 162.11, 143.39, 129.5, 124.42, 61.1, 60.65. ESI-MS: *m/z* 271 [M^{2+}-H] (calculated for [$C_{16}H_{20}N_2O_2^{2+}$-H] 271.15.). EA: calculated 44.47% C, 4.66% H, 6.48% N; found 44.62% C, 4.9% H, 6.3% N.

but-(2E)-en-1,4-diyl-1,1′-bis(4-(3-hydroxypropyl)pyridinium) dibromide (14)

Mp 171–173°C. Yield 69 %. ^{1}H NMR (300 MHz, DMSO d_6): δ (ppm) 8.96 (d, 4H, J=5.8 Hz, H–2,2′,6,6′), 8.06 (d, 4H, J=5.8 Hz, H–3,3′,5,5′), 6.21–6.16 (m, 2H, =*CH*-), 5.32–5.28 (m, 4H, -CH_2-), 3.43 (t, 4H, J=6.2 Hz, -CH_2-OH), 2.9 (t, 4H, J=7.6 Hz, -CH_2-N), 1.81 (m, 4H, -CH_2-CH_2-N). ^{13}C NMR (75 MHz, DMSO d_6): δ (ppm) 143.98, 130.07, 127.7, 59.94, 59.53. ESI-MS: *m/z* 327.9 [M^{2+}] (calculated for [$C_{20}H_{28}N_2O_2^{2+}$] 328.21). EA: calculated 49.2% C, 5.78% H, 5.74% N; found 48.87% C, 6% H, 6.01% N.

but-(2E)-en-1,4-diyl-1,1′-bis(4-(N,N-dimethylamino)-pyridinium) dibromide (15)

Mp decomp 314°C. Yield 68 %. ^{1}H NMR (300 MHz, DMSO d_6): δ (ppm) 7.94 (d, 4H, J = 6.7 Hz, H–2,2′,6,6′), 6.82 (d, 4H, J = 6.7 Hz, H–3,3′,5,5′), 5.88–5.84 (m, 2H, =*CH*-), 4.7–4.66 (m, 4H, -CH_2-), 3.07 (s, 12H, N-CH_3). ^{13}C NMR (75 MHz, DMSO d_6): δ (ppm) 157.08, 142.53, 130.57, 108.77, 58.57, 40.75. ESI-MS: *m/z* 297.9 [M^{2+}] (calculated for [$C_{18}H_{26}N_4^{2+}$] 298.21). EA: calculated 47.18% C, 5.72% H, 12.23% N; found 47.12% C, 6.04% H, 12.15% N.

but-(2E)-en-1,4-diyl-1,1′-bis(4-hydroxyiminomethylpyridinium) dibromide (16)

Mp 232–234°C. Yield 95%. Further physic-chemical data are consistent with the literature [20].

but-(2E)-en-1,4-diyl-1,1′-bis(4-methylcarbonylpyridinium) dibromide (17)

Mp 228–230°C. Yield 56 %. ^{1}H NMR (300 MHz, DMSO d_6): δ (ppm) 9.36 (d, 4H, J=5.6 Hz, H–2,2′,6,6′), 8.54 (d, 4H, J=5.8 Hz, H–3,3′,5,5′), 6.32–6.26 (m, 2H, =*CH*-), 5.53–5.47 (m, 4H, -CH_2-), 2.76 (s, 6H, -CH_3). ^{13}C NMR (75 MHz, DMSO d_6): δ (ppm) 195.67, 148.63, 146.39, 130.21, 125.92, 60.87, 27.49. ESI-MS: *m/z* 296.0 [M^{2+}] (calculated for [$C_{18}H_{20}N_2O_2^{2+}$] 296.15). EA: calculated 47.39% C, 4.42% H, 6.14% N; found 47.51% C, 4.66% H, 5.97% N.

but-(2E)-en-1,4-diyl-1,1′-bis(4-carboxypyridinium) dibromide (18)

Mp 274–276°C. Yield 35 %. ^{1}H NMR (300 MHz, DMSO d_6): δ (ppm) 9.27 (d, 4H, J=5.9 Hz, H–2,2′,6,6′), 8.51 (d, 4H, J=5.9 Hz, H–3,3′,5,5′), 6.27–6.22 (m, 2H, =*CH*-), 5.5–5.45 (m, 4H, -CH_2-). ^{13}C NMR (75 MHz, DMSO d_6): δ (ppm) 146.3, 145.61, 130.18, 127.31, 61.03. ESI-MS: *m/z* 299.7 [M^{2+}] (calculated for [$C_{16}H_{16}N_2O_4^{2+}$] 300.11). EA: calculated 41.77% C, 3.5% H, 6.09% N; found 41.44% C, 3.8% H, 6.29% N.

but-(2E)-en-1,4-diyl-1,1′-bis(4-methyloxycarbonylpyridinium) dibromide (19)

Mp 179–181°C. Yield 80 %. ^{1}H NMR (300 MHz, DMSO d_6): δ (ppm) 9.33 (d, 4H, J=5.8 Hz, H–2,2′,6,6′), 8.54 (d, 4H, J=5.6 Hz, H–3,3′,5,5′), 6.29–6.24 (m, 2H, =*CH*-), 5.54–5.47 (m, 4H, N-CH_2-), 4.45 (q, 4H, J=7 Hz, O-CH_2-), 1.37 (t, 6H, J=7 Hz, O-CH_2-CH_3). ^{13}C NMR (75 MHz, DMSO d_6): δ (ppm) 161.95, 146.43, 144.12, 130.18, 127.15, 62.93, 61.07, 13.81. ESI-MS: *m/z* 328 [M^{2+}] (calculated for [$C_{18}H_{20}N_2O_4^{2+}$] 328.14). EA: calculated 44.29% C, 4.13% H, 5.74% N; found 44.45% C, 3.93% H, 5.55% N.

but-(2E)-en-1,4-diyl-1,1′-bis(4-carbamoylpyridinium) dibromide (20)

Mp 268–270°C. Yield 90 %. ^{1}H NMR (300 MHz, DMSO d_6): δ (ppm) 9.28 (d, 4H, J = 5.5 Hz, H–2,2′,6,6′), 8.75 (s, 2H, -CONH_2), 8.48 (d, 4H, J = 5.6 Hz, H–3,3′,5,5′), 8.31 (s, 2H, -CONH_2), 6.28–6.21 (m, 2H, =*CH*-), 5.48–5.39 (m, 4H, -CH_2-). ^{13}C NMR (75 MHz, DMSO d_6): δ (ppm) 163.19, 148.39, 145.89, 130.1, 125.86, 60.82. ESI-MS: *m/z* 298 [M^{2+}] (calculated for [$C_{16}H_{18}N_4O_2^{2+}$] 298.14). EA: calculated 41.95% C, 3.96% H, 12.23% N; found 41.85% C, 3.8% H, 12.32% N.

but-(2E)-en-1,4-diyl-1,1′-bis(4-carbonitrilpyridinium) dibromide (21)

Mp 251–253°C. Yield 46 %. ^{1}H NMR (300 MHz, DMSO d_6): δ (ppm) 9.02 (d, 4H, *J* = 6.1 Hz, H–2,2′,6,6′), 8.38 (d, 4H, *J* = 6.1 Hz, H–3,3′,5,5′), 6.25–6.21 (m, 2H, =*CH*-), 5.32–5.28 (m, 4H, -CH_2-). ^{13}C NMR (75 MHz, DMSO d_6): δ (ppm) 147.17, 132.54, 131.39, 129.63, 115.56, 63.78. ESI-MS: *m/z* 262 [M^{2+}] (calculated for [$C_{16}H_{14}N_4^{2+}$] 262.12). EA: calculated 45.53% C, 3.34% H, 13.27% N; found 45.63% C, 3.26% H, 13.24% N.

In vitro assay

A multichannel Sunrise spectrophotometer (Tecan, Salzburg, Austria) was used for all measurements of cholinesterases activity. An optimised Ellman's procedure was slightly adapted in order to estimate the anticholinergic properties [21]. Some 96-well photometric microplates made from polystyrene (Nunc, Rockilde, Denmark) were used for measuring purposes. Human erythrocyte AChE or human plasmatic BChE (Prague, Aldrich; commercially purified by affinity chromatography) were suspended into phosphate buffer (pH 7.4) up to a final activity of 0.002 U/μL. Cholinesterase (5 μL), freshly mixed solution of 0.4 mg/mL 5,5′-dithio-bis(2-nitrobenzoic) acid (40 μL), 1 mM acetylthiocholine chloride in phosphate buffer (20 μL) and the appropriate concentration of the inhibitor (1 mM–0.1 nM; 5 μL) were injected into each well. The absorbance was measured at 412 nm after 5 minutes incubation using automated shaking of the microplate. All measurements were performed in triplicate.

The percentage inhibition (I) was calculated from the measured data as follows:

$$\mathrm{I} = 1 - \frac{\Delta A_i}{\Delta A_0}$$

where ΔAi indicates the absorbance change provided by cholinesterase exposed to an anticholinergic compound. ΔA_0 indicates the absorbance change caused by the intact cholinesterase, where phosphate buffer was applied instead of the anticholinergic compound.

The IC_{50} was determined using the software package Origin 6.1 (Northampton, MA, USA). The percentage inhibition was calculated by a Hill plot (n = 1). The other plot variants were not optimal and their correlation coefficients were lower compared to the chosen method. Subsequently, the IC_{50} was computed.

Enzyme kinetics assay

Human erythrocyte AChE (Aldrich) was used throughout the experiments. The adapted photometrical Ellman's method was used to evaluate the AChE activity [22]. A polystyrene cuvette was filled with 0.4 mg/ml DTNB (0.4 ml), AChE solution with an overall activity of 0.5 μkat (μmol/s) in phosphate buffered saline (PBS; 25 μL), tested inhibitor (25 μL), and PBS (450 μL). The mixture was gently shaken and the reaction was started by addition of varying concentration (0.1 mM–1 M) of ATChCl in PBS (100 μL). The yellow colour produced by the 5-thio-2-nitrobenzoic acid was measured at 412 nm against a control blank (mixture of DTNB and ATChCl in given concentrations). The spontaneous interaction between the tested inhibitor and DTNB was excluded after incubation of the whole reaction mixture without AChE that was replaced by PBS (25 μL). The inhibition was evaluated by a Lineweaver-Burk plot for all inhibitor concentrations (10^{-8}–10^{-2} mol/L) and ATChCl concentrations (10^{-5}–10^{-1} mol/L). The measurements were carried out in triplicate and the average value was used for the plot construction.

The obtained data were processed by Origin 8.0 software (Northampton, MA, USA). The constants were calculated from the enzyme kinetics using a Lineweaver-Burk plot (double reciprocal plot). The AChE dissociation constant for the enzyme-inhibitor complex (K_{i1}) and the dissociation constant for the enzyme–inhibitor–substrate complex (K_{i2}) were calculated using the following equations:

$$K_{i1} = \frac{[E][I]}{[EI]}$$

$$K_{i2} = \frac{[ES][I]}{[ESI]}$$

Molecular docking

The docking calculations were carried out using Autodock 4.0.1 [23]. The structure of *mus musculus* AChE and human AChE were prepared from the crystal structure (pdb code 2jez, 2jf0 and 1b41) using the Autodock Tools 1.5.2 [23]. The 3D affinity grid box was designed to include both the full active and the peripheral site of AChE. The number of grid points in the x-, y- and z-axes was 110, 110 and 110 with grid points separated by 0.253 Å. The molecular models of ligands were built using ChemDraw 11.1 and minimised with UCSF Chimera 1.3 (Amber Force field) in the charged form [24]. Docking calculations were set to 50 runs. A population of 150 individuals and 2 500 000 function evaluations were used. The structure optimisation was performed for 27 000 generations using a genetic algorithm. The maximum root mean square tolerance for the conformational cluster analysis was 2 Å. At the end of calculation, the Autodock performed cluster analysis was utilised. The visualisations of the enzyme-ligand interactions (Figure 3 and Figure 4) were prepared using Pymol 1.1 [25].

Results and discussion

In vitro results

The bisquaternary compounds were assayed for their inhibitory ability using a standard inhibition test utilising human erythrocyte AChE (hAChE) and human plasmatic BChE (hBChE) [21]. The hAChE was chosen as the main target for the OP pre-treatment [11]. Additionally,

hBChE was chosen as a member of the cholinesterase family, which is usually affected by all the compounds that interact with AChE [26]. The IC_{50} values of all compounds are listed in Table I.

Based on the inhibition of hAChE, the commercial compound **1** presented a satisfactory inhibition of AChE in the μM range. In contrast, compound **2** was a stronger inhibitor of hAChE and had an IC_{50} approximately three orders of magnitude lower compared to **1**. From these *in vitro* results, compound **2** appears to be a potentially more valuable inhibitor of hAChE between these two tested carbamate compounds. The AChE reactivators are also known for their inhibitory ability towards AChE [27] as some of them were found to be potent AChE reactivators/inhibitors *in vitro* [28]. However, both the tested reactivators (**3**, **4**) presented only a minor inhibition of hAChE that probably limits their use in pre-exposure treatment as functional AChE inhibitors. Therefore their potential receptor mediated protection against OP should be further studied.

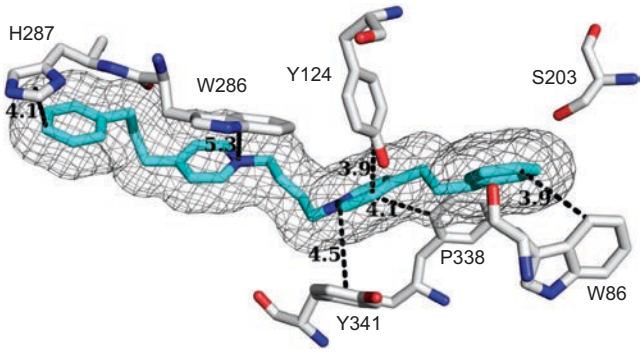

Figure 3. Docking results for compound **10** with hAChE.

Among the newly prepared compounds (**3**–**19**), the inhibitory ability towards hAChE greatly varied within the whole series. One novel compound (**7**) was not soluble in the screening solution and consequently could not be evaluated. Two compounds (**16, 18**) showed negligible inhibition on a mM scale. Some compounds (**4**, **6**, **9**–**12**, **14**–**15**, **17**, **19**) showed inhibition on a less than mM scale, but did not exceed the standard carbamate inhibitor **1**. More interestingly, four compounds (**3**, **5**, **8**, **13**) presented an inhibitory ability comparable (**5**) or better (**3**, **8**, **13**) than the standard carbamate **1**. In addition, one newly prepared compound (**8**) showed an inhibition of hAChE on a nM scale and exceeded both carbamate inhibitors **1** and **2**.

For hBChE, the commercial compound **1** was found to be a very poor inhibitor. Interestingly, a second carbamate compound (**2**) showed a strong inhibition of hBChE on a less than μM scale and about 5 orders of magnitude

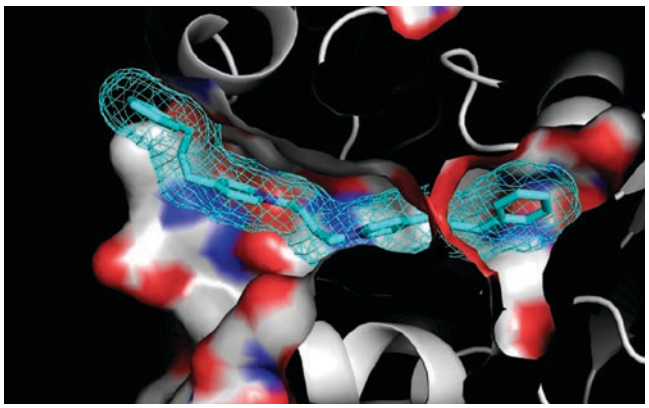

Figure 4. Penetration of compound **10** into the the hAChE active site gorge.

Table 1. The IC_{50} values of the tested compounds (a; no inhibition observed; b; not soluble in screening medium).

Compound	AChE IC_{50} ± SD (μM)	BChE IC_{50} ± SD (μM)	K_{i1}/K_{i2} (μM)
pyridostigmine (**1**)	40 ± 7.8	16 000 ± 260.8	4.94/2.52
neostigmine(**2**)	0.1 ± 0.02	0.8 ± 0.13	0.44/0.07
pralidoxime (**3**)	878 ± 171	a	---
K203 (**4**)	566 ± 110	3 130 ± 510	---
5	0.9 ± 0.2	a	---
6	212 ± 41	850 ± 138	---
7	40 ± 8	169 ± 28	---
8	71 ± 14	18 ± 3	---
9	b	b	---
10	0.05 ± 0.01	22 ± 4	0.003/0.009
11	73 ± 14	18 ± 3	---
12	509 ± 99	a	---
13	799 ± 155	4 510 ± 735	---
14	54 ± 11	1 440 ± 234	---
15	1.2 ± 0.2	17 ± 3	---
16	189 ± 37	1 620 ± 264	---
17	139 ± 27	324 ± 53	---
18	3 870 ± 754	a	---
19	401 ± 78	a	---
20	1 200 ± 234	a	---
21	70 ± 14	514 ± 84	---

better than **1**. The AChE reactivators (**3**, **4**) were negligible inhibitors of hBChE. Among the newly prepared compounds (**3**–**19**), the inhibitory ability towards hBChE greatly varied within the whole series. One novel compound (**7**) was not soluble in the screening solution and consequently could not be further evaluated. Several novel compounds (**3**, **10**, **16**–**18**) showed no inhibition of hBChE activity. Three compounds (**11**–**12**, **14**) were negligible inhibitors at the mM scale and four compounds (**4**–**5**, **15**, **19**) were poor inhibitors on a less than mM scale. More interestingly, several newly prepared compounds (**6**, **8**–**9**, **13**) showed inhibition at the μM scale. However, the novel compounds were not able to exceed the carbamate **2** at hBChE inhibition.

The IC_{50} screening method provides a complex comparison between inhibitors because of their different inhibition mechanisms, and so the kinetics data were measured for specific compounds of interest. The dissociation constants (K_{i1} and K_{i2}) were calculated for 2 carbamate standards (**1**, **2**) and for the most promising compound (**8**) interacting with hAChE [22]. In all cases, a non-competitive mechanism of inhibition was confirmed by the shape of the Lineweaver-Burk plot. For pyridostigmine (**1**), the inhibition constants differed approximately two fold (K_{i1} = 4.94 μmol/l; K_{i2} = 2.52 μmol/l), where the substrate presence increased the inhibition of AChE (decreased the inhibition constant). The kinetic constants for neostigmine (**2**) differed about six fold (K_{i1} = 0.44 μmol/l; K_{i2} = 0.07 μmol/l) and the presence of the substrate again increased the inhibition of AChE. The inhibition constants of compound **8** (K_{i1} = 0.003 μmol/l; K_{i2} = 0.009 μmol/l) differed only slightly, where the presence of the substrate decreased the inhibitory ability of compound **8** towards AChE. Importantly, both K_i values of compound **8** were found to be at least one order of magnitude lower compared to the tested standards (**1**, **2**).

Molecular docking and SAR results

The docking study was performed on the most promising compound after the *in vitro* screening (**8**) in order to rationalise the possible interactions within the main enzyme of interest (AChE) [29]. Three crystal structures were used for the docking calculations (hAChE – 1b41, mAChE – 2jez, 2jf0) and the best results were obtained for a hAChE model (1b41) [30]. It was found that the top scoring docking pose of compound **8** (–9.66 kcal/mol) showed apparent interactions with the aromatic residues of an internal anionic site (IAS) and a peripheral anionic site (PAS) (Figure 3) [31]. Specifically, a π-π interaction occurred between one phenyl moiety and Trp86 (3.9 Å) from the IAS. One pyridinium ring showed T-stacking both with Tyr124 (3.9 Å) and Phe338 (4.1 Å) and a weak π-π or cation-π interaction with Tyr341 (4.5 Å) from PAS. A second pyridinium ring displayed a long distance from the Trp286 (5.3 Å), but the second phenyl moiety presented a π-π interaction with His287 (4.1 Å). Besides the aromatic interactions, inhibitor **8** did not display any interactions with the hAChE catalytic site (S203) as might have been hypothesised from its chemical structure. Inhibitor **8** also showed a good penetration of the one 4-(3-phenylpropyl)-pyridinium moiety into the hAChE active site (Figure 4).

The SAR results of the novel synthesised compounds originated from the docking study and the *in vitro* data [32]. Since the but-(2*E*)-en-1,4-diyl-bispyridinium structure remained the same for all the novel compounds, the main part of the molecule influencing the SAR from the various functional groups attached to the pyridinium moieties were at the 4-position.

For hAChE, the lipophilic moieties (**3**–**9**) suggested that they are very promising inhibitors. The aliphatic functional groups (**3**–**5**) showed interesting differences in the inhibitory ability, where the methyl moiety (**3**) was superior to *tert*.-butyl (**5**) or the ethyl (**4**). Among the aromatic functional groups (**6**–**9**), 3-phenylpropyl compound (**8**) was found to be the best inhibitor from the prepared series, superior to phenyl (**6**) or 4-nitrobenzyl (**9**), on account of the valuable π-π or cation-π interactions with the aromatic residues of AChE (i.e. His, Phe, Trp, Tyr) [33]. The benzyl compound (**7**) remained insoluble, but introduction of a hydrophilic 4-nitro moiety, resulting in 4-nitrobenzyl (**9**), showed good solubility and inhibitory ability to the same level as the phenyl compound (**6**). The hydrophilic moieties (**10**–**19**) also showed apparent differences in their inhibitory ability. Among them, 3-hydroxypropyl (**12**), *N,N*-dimethylamino (**13**) and 4-carbonitril (**19**) were superior to the other hydroxy (**10, 11**) and carbonyl compounds (**14**–**18**). Though the *N,N*-dimethylamino compound (**13**) tested as the best hydrophilic moiety, its inhibitory ability was still two orders of magnitude lower as compared to the 3-phenylpropyl compound (**8**).

For hBChE, the SAR extensively changed. Among the lipophilic molecules (**3**–**9**), the phenyl (**6**), 3-phenylpropyl (**8**) and 4-nitrobenzyl (**9**) compounds showed a similar inhibitory ability. The benzyl compound (**7**) remained insoluble, but introduction of a hydrophilic 4-nitro moiety, resulting in 4-nitrobenzyl (**9**), showed good solubility and an inhibitory ability similar to the phenyl compound (**6**). The aliphatic moieties (**3**–**5**) presented minor inhibition of hBChE. In contrast to hAChE, the methyl compound (**3**) did not inhibit hBChE. The hydrophilic moieties (**10**–**19**) also showed differences in their inhibitory ability towards hBChE. The hydroxy (**10**), carboxy (**16**), methyloxycarbonyl (**17**) and carbamoyl (**18**) moieties did not show inhibition of hBChE. The *N,N*-dimethylamino compound (**13**) was found to be superior to all the other hydroxy (**11**, **12**) and carbonyl compounds (**14**, **15, 19**), and its inhibitory ability towards hBChE was comparable to the best lipophilic moieties (**6**, **8**, **9**).

The selectivity between AChE and BChE is another necessary factor for suitable future SAR determination and further development. In this study, two compounds

(**5, 10**) were found to be greater than three orders of magnitude more potent inhibitors of AChE. Though their moieties are different, it can be hypothesised why such moieties tested so well. The selectivity of compound **5** with a methyl moiety was probably caused by its small spatial size, thereby helping this compound to be accommodated in the spatially restricted AChE active site. Regarding BChE, compound **5** was probably unable to interact with its active site as it does not have the aromatic residues similar to the PAS of AChE [34]. The selectivity of compound **10** with a 3-phenylpropyl moiety towards AChE was confirmed by the docking results, where many π-π or cation-π interactions were possible. In the case of BChE, many aromatic residues were absent and so compound **10** could not interact with this enzyme on a similar basis as with AChE.

The valuable SAR features for quaternary cholinesterase inhibitors can be defined. The bispyridinium origin of these novel compounds established their high affinity for cholinesterases. In addition, spatially narrow molecules (e.g. containing a (2*E*)-buten-1-,4-diyl linker) might help access to the AChE active site. However, these interactions also depend upon the other moieties carried on the pyridinium ring: small moieties (e.g. methyl) were found to be suitable for the selective inhibition of AChE due to its small spatial size. Similarly, the aromatic moieties (e.g. 3-phenylpropyl) were found to be convenient and selective inhibitors due to their π-electron interactions with the AChE active site.

Conclusion

In summary, seventeen bisquaternary cholinesterase inhibitors were prepared. They were evaluated *in vitro* on the human erythrocyte AChE and the human plasmatic BChE with regard to their IC_{50} results. The *in vitro* data were compared to currently used carbamate inhibitors (pyridostigmine bromide, neostigmine bromide) and also AChE reactivators (pralidoxime, K203). One novel compound (**10**) was found to be better than the currently known compounds at inhibiting hAChE activity. The kinetic assay confirmed the non-competitive inhibition of hAChE by this leading novel compound. The molecular docking of this compound confirmed the apparent influence of both π-π and cation-π interactions within the AChE active site to help explain its increased inhibitory ability.

Acknowledgements

The authors express their appreciation to Petr Stodulka for technical assistance.

Declaration of interest

This work was supported by the Grant Agency of the Ministry of Defence Czech Republic No. OVUOFVZ200805 and by the Grant Agency of the Charles University No. 117909/2009/B-CH/FaF.

References

1. Marlatt MW, Webber KM, Moreira PI, Lee HG, Casadesus G, Honda K, Zhu XW, Perry G, Smith MA. Therapeutic opportunities in Alzheimer disease: One for all or all for one? Curr Med Chem 2005;12:1137–1147.
2. Garcia-Carrasco M, Escarcega RO, Fuentes-Alexandro S, Riebeling C, Cervera R. Therapeutic options in autoimmune myasthenia gravis. Autoimmun Rev 2007;6:373–378.
3. Patocka J, Kuca K, Jun D. Acetylcholinesterase and butyrylcholinesterase-- important enzymes of human body. Acta Medica 2004;47:215–228.
4. Marrs TC. Organophosphate poisoning. Pharmacol Therap 1993;58:51–66.
5. Bajgar J. Organophosphates/nerve agent poisoning: mechanism of action, diagnosis, prophylaxis, and treatment. Adv Clin Chem 2004;38:151–216.
6. Doctor BP, Raveh L, Wolfe AD, Maxwell DM, Ashani Y. Enzymes as pretreatment drugs for organophosphate toxicity. Neurosci Biobehav Rev 1991;15:123–128.
7. Bajgar J, Fusek J, Kassa J, Kuca K, Jun D. Chemical aspects of pharmacological prophylaxis against nerve agent poisoning. Curr Med Chem 2009;16:2977–2986.
8. Sultatos LG. Interactions of organophosphorus and carbamate compounds with cholinesterases, In: Gupta RC, ed. Toxicology of Organophosphate and Carbamate Compounds. London: Elsevier Academic Press; 2006:209–218.
9. Beck KD, Zhu G, Beldowicz D, Brennan FX, Ottenweller JE, Moldow RL, Servatius RJ. Central nervous system effects from a peripherally acting cholinesterase inhibiting agent: interaction with stress or genetics. Ann N Y Acad Sci 2001;933:310–314.
10. Peden-Adams MM, Dudley AC, EuDaly JG, Allen TC, Gilkeson GS, Keil DE. Pyridostigmine bromide (PYR) alters immune function in B6C3F1 mice. Immunopharm Immunot 2004;26:1–15.
11. Bajgar J. Complex view on poisoning with nerve agents and organophosWphates. Acta Medica 2005;48:3–21.
12. Soukup O, Tobin G, Kumar UK, Binder J, Proska J, Jun D, Fusek J, Kuca K. Interaction of nerve agent antidotes with cholinergic systems. Curr Med Chem 2010;17:1708–1718.
13. Musilek K, Kuca K, Jun D, Dohnal V, Dolezal M. Synthesis of the novel series of bispyridinium compounds bearing (E)-but-2-ene linker and evaluation of their reactivation activity against chlorpyrifos-inhibited acetylcholinesterase. Bioorg Med Chem Lett 2006;16:622–627.
14. Musilek K, Jun D, Cabal J, Kassa J, Gunn-Moore F, Kuca K. Design of a potent reactivator of tabun-inhibited acetyleholinesterase-synthesis and evaluation of (E)-1-(4-carbamoylpyridinium)-4-(4-hydroxyiminomethylpyridinium)-but-2-ene dibromide (K203). J Med Chem 2007;50:5514–5518.
15. Musilek K, Holas O, Kuca K, Jun D, Dohnal V, Opletalova V, Dolezal M. Synthesis of monooxime-monocarbamoyl bispyridinium compounds bearing (E)-but-2-ene linker and evaluation of their reactivation activity against tabun- and paraoxon-inhibited acetylcholinesterase. J Enzyme Inhib Med Chem 2008;23:70–76.
16. Musilek K, Holas O, Jun D, Dohnal V, Gunn-Moore F, Opletalova V, Dolezal M, Kuca K. Monooxime reactivators of acetylcholinesterase with (E)-but-2-ene linker - Preparation and reactivation of tabun- and paraoxon-inhibited acetylcholinesterase. Bioorg Med Chem 2007;15:6733–6741.
17. Sussman JL, Harel M, Frolow F, Oefner C, Goldman A, Toker L, Silman I. Atomic-structure of acetylcholinesterase from *Torpedo-californica*-A prototypic acetylcholine-binding protein. Science 1991;253:872–879.
18. Musilek K, Komloova M, Zavadova V, Holas O, Hrabinova M, Pohanka M, Dohnal V, Nachon F, Dolezal M, Kuca K, Jung Y-S.

Preparation and *in vitro* screening of symmetrical bispyridinium cholinesterase inhibitors bearing different connecting linkage – initial study for Myasthenia gravis implications. Bioorg Med Chem Lett 2010;20:1763–1766.
19. Musilek K, Holas O, Kuca K, Jun D, Dohnal V, Dolezal M. Synthesis of a novel series of non-symmetrical bispyridinium compounds bearing a xylene linker and evaluation of their reactivation activity against tabun and paraoxon-inhibited acetylcholinesterase. J Enzyme Inhib Med Chem 2007;22:425–432.
20. Kuca K, Cabal J, Musilek K, Jun D, Bajgar J. Effective bisquaternary reactivators of tabun-inhibited AChE. J Appl Toxicol 2005;25:491–495.
21. Pohanka M, Jun D, Kuca K. Improvement of acetylcholinesterase-based assay for organophosphates in way of identification by reactivators. Talanta 2008;77:451–454.
22. Pohanka M, Hrabinova M., Kuca K. Diagnosis of intoxication by the organophosphate VX: Comparison between an electrochemical sensor and Ellman's photometric method. Sensors 2008;8:5229–5237.
23. Morris GM, Goodsell DS, Halliday RS, Huey R, Hart WE, Belew RK, Olson AJ. Automated docking using a Lamarckian genetic algorithm and an empirical binding free energy function. J Comput Chem 1998;19:1639–1662.
24. Pettersen EF, Goddard TD, Huang CC, Couch GS, Greenblatt DM, Meng EC, Ferrin TE. UCSF chimera - A visualization system for exploratory research and analysis. J Comput Chem 2004;25:1605–1612.
25. DeLano WL. The PyMOL Molecular Graphics System (2002) on the World Wide Web http://www.pymol.org
26. Masson P, Carletti E, Nachon F. Structure, activities and biomedical applications of human butyrylcholinesterase. Prot Pept Lett 2009;16:1215–1224.
27. Petroianu GA, Arafat K, Kuca K, Kassa J. Five oximes (K-27, K-33, K-48, BI-6 and methoxime) in comparison with pralidoxime: *in vitro* reactivation of red blood cell acetylcholinesterase inhibited by paraoxon. J Appl Toxicol 2006;26:64–71.
28. Lorke DE, Hasan MY, Arafat K, Kuca K, Musilek K, Schmitt A, Petroianu GA. *In vitro* oxime protection of human red blood cell acetylcholinesterase inhibited by diisopropyl-fluorophosphate. J Appl Toxicol 2008;28:422–9.
29. Leonetti F, Catto M, Nicolotti O, Pisani L, Cappa A, Stefanachi A, Carotti A. Homo- and hetero-bivalent edrophonium-like ammonium salts as highly potent, dual binding site AChE inhibitors. Bioorg Med Chem 2008;16:7450–7456.
30. www.pdb.org
31. Johnson G, Moore SW. The peripheral anionic site of acetylcholinesterase: structure, functions and potential role in rational drug design. Curr Pharm Des 2006;12:217–225.
32. Kuca K, Jun D, Musilek K. Structural requirements of acetylcholinesterase reactivators. Mini Rev Med Chem 2006;6:269–277.
33. Ma JC, Dougherty DA. The cation-pi interaction. Chem Rev 1997;97:1303–1324.
34. Wiesner J, Kriz Z, Kuca K, Jun, D, Koca J. Why acetylcholinesterase reactivators do not work in butyrylcholinesterase. J Enzyme Inhib Med Chem 2010;25:318–322.